Dear Author

Please use this PDF proof to check the layout of your article. If you would like any changes to be made to the layout, you can leave instructions in the online proofing interface. First, return to the online proofing interface by clicking "Edit" at the top page, then insert a Comment in the relevant location. Making your changes directly in the online proofing interface is the quickest, easiest way to correct and submit your proof.

Please note that changes made to the article in the online proofing interface will be added to the article before publication, but are not reflected in this PDF proof.

If you would prefer to submit your corrections by annotating the PDF proof, please download and submit an annotatable PDF proof by clicking the link below.

Annotate PDF

AUTHOR QUERY FORM

AIP Publishing	Journal: Rev. Sci. Instrum. Article Number: RSI23-AR-02290	Please provide your responses and any corrections by annotating this PDF and uploading it to AIP's eProof website as detailed in the Welcome email.

Dear Author,

Below are the queries associated with your article. Please answer all of these queries before sending the proof back to AIP.

Article checklist: In order to ensure greater accuracy, please check the following and make all necessary corrections before returning your proof.
1. Is the title of your article accurate and spelled correctly?
2. Please check affiliations including spelling, completeness, and correct linking to authors.
3. Did you remember to include acknowledgment of funding, if required, and is it accurate?

Location in article	Query/Remark: click on the Q link to navigate to the appropriate spot in the proof. There, insert your comments as a PDF annotation.
Q1	Please check that the author names are in the proper order and spelled correctly. Also, please ensure that each author's given and surnames have been correctly identified (given names are highlighted in red and surnames appear in blue).
Q2	We have reworded the sentence beginning "To quantify the impact of the shift ..." for clarity. Please check that your meaning is preserved.
Q3	Figure 5 was not cited in the text. We have inserted a citation in the sentence beginning "Any transverse misalignment. . .." Please check and reposition if necessary.
Q4	Please provide a data availability statement for your paper.
Q5	If e-print Ref. 10 has subsequently been published elsewhere, please provide updated reference information (journal title, volume number, and page number).
	Please confirm ORCIDs are accurate. If you wish to add an ORCID for any author that does not have one, you may do so now. For more information on ORCID, see https://orcid.org/. Florentin Adam – 0009-0006-3356-9916 Wen Xin Chiew – 0009-0004-1379-9242 Adrian Nugraha Utama – 0009-0005-0759-6753 Christian Kurtsiefer – 0000-0003-2190-0684
	Please check and confirm the Funder(s) and Grant Reference Number(s) provided with your submission: National Research Foundation Singapore, Award/Contract Number NRF2021-QEP2-01-P01/W21Qpd0101 Please add any additional funding sources not stated above.

Thank you for your assistance.

Review of Scientific Instruments ARTICLE pubs.aip.org/aip/rsi

Low noise near-concentric optical cavity design

Cite as: Rev. Sci. Instrum. 95, 000000 (2024); doi: 10.1063/5.0191123
Submitted: 11 December 2023 • Accepted: 24 March 2024 •
Published Online: 9 99 9999

View Online Export Citation CrossMark

Florentin Adam,[1] Wen Xin Chiew,[1] Adrian Nugraha Utama,[1] and Christian Kurtsiefer[1,2,a)]

AFFILIATIONS

[1] Center for Quantum Technologies, 3 Science Drive 2, Singapore 117543
[2] Department of Physics, National University of Singapore, 2 Science Drive 3, Singapore 117542

[a)] **Author to whom correspondence should be addressed:** christian.kurtsiefer@gmail.com

ABSTRACT

Near-concentric cavities are excellent tools for enhancing an atom–light interaction as they combine a small mode volume with a large optical access for atom manipulation. However, they are sensitive to longitudinal and transverse misalignments. To address this sensitivity, we present a compact near-concentric optical cavity system with a residual cavity length variation $\delta L_{C,rms} = 0.36(2)$ Å. A key part of this system is a cage-like tensegrity mirror support structure that allows us to correct for longitudinal and transverse misalignments. The system is stable enough to allow the use of mirrors with a higher cavity finesse to enhance the atom–light coupling strength in cavity-QED applications.

INTRODUCTION

Establishing a strong atom–light interaction is essential for the implementation of quantum networks in atomic systems.[1,2] However, interfacing with atoms can be challenging due to their small cross section. Commonly used approaches to enhance the atom–light interaction involve highly focusing lenses[3] or optical resonators.[4] For the latter, cavity quantum electrodynamics (CQED) has extensively been researched with optical resonators in various configurations[5] and demonstrated with single atoms since the 1980s.[6,7] To attain a strong atom–light coupling strength g, typically short cavities with a small mode volume and high reflectivity, low loss mirrors are used. This leads to atom–light interactions using cavity mirror spacings ranging from micrometers[8,9] to millimeters[10] with a high quality factor Q. Most of the cavities for CQED involve a near-planar geometry, with a mirror separation much smaller than their radius of curvature. This allows for stable mechanical designs but requires a short distance between the mirror surfaces.

Optical cavities in the near-concentric (NC) regime, where the length of the cavity is close to the sum of the spherical mirrors' radii of curvature, have most of the cavity modes strongly focused at the center, leading to a small effective mode volume[11,12] and thus a strong atom–light coupling strength g while providing easy optical access through the relatively large mirror separation.

However, NC cavities are challenging to work with compared to planar micro-cavities, as the transverse displacement of the mirrors affects the cavity resonance. As the optical cavity resonance needs to have a well-defined relation to fixed atomic resonances in CQED applications, the mechanical cavity stability is critical. In NC cavities, there is an additional requirement for transverse adjustability and stability, leading to the need for control of three degrees of freedom for relative mirror positions.

Here, we present a NC configuration of an optical resonator exhibiting low susceptibility to external mechanical noise and thus stability, while maintaining adjustability in all necessary degrees of freedom, allowing us to operate the cavity close to the concentric point and hence explore a stronger atom–light coupling.

CAVITY DESIGN

To facilitate an atom–cavity interaction at a specific transition, in our case, the D_2 line of ^{87}Rb at $\lambda = 780$ nm with an atomic half-linewidth $\gamma = 2\pi \times 3.03$ MHz, the cavity resonance frequency ω_C has to match with the atomic resonance frequency. In addition, as ^{87}Rb atoms are to be trapped at the cavity center using a magneto-optical trap[13] and a dipole trap[14] in an ultra-high-vacuum (UHV) environment, optical access to the system is necessary. To minimize the size of magnetic coils, a small glass cuvette with inside dimensions of $25 \times 25 \times 150$ mm^3 is used.

Stability requirement

To quantify the impact of the shift in cavity resonance and the cavity performance, we introduce a "noise limit factor" ξ, which normalizes the ratio of the frequency fluctuation $\delta\omega_C$ due to mechanical noise to the cavity linewidth 2κ. This factor is equivalent to the ratio

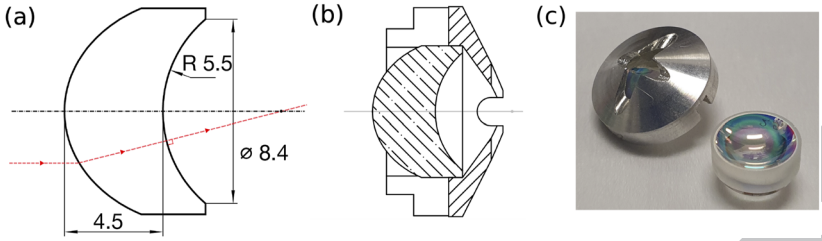

FIG. 1. Schematic of the cavity mirror: (a) with an example of ray propagation in red through the mirror (units in mm), (b) with the mirror mount, and (c) corresponding pictures.

of the mechanical noise (standard deviation δL_C of the cavity length) to the resonant wavelength, multiplied by the cavity finesse F,

$$\xi = \frac{\delta\omega_C}{2\kappa} = \frac{\delta L_C}{\lambda/2} F. \tag{1}$$

A noise limit factor $\xi = 1$ indicates that the cavity resonance fluctuation is equal to its linewidth. Here, we aim for a target of $\xi = 0.15$, which means that the mechanical noise along the cavity axis contributes to the cavity linewidth by at most 15%.

Both transverse and longitudinal misalignments will affect the reflection and/or transmission of the NC cavity. Close to the concentric point, the cavity becomes increasingly sensitive to transverse displacement. This heightened sensitivity leads to fluctuations in cavity resonance and transmission and requires addressing transverse stabilization in the cavity structure. For convenience, we map all mechanical effects on the cavity resonance to the effective fluctuation of the cavity length δL_C.

Mirror characteristics

The cavity mirrors (see Fig. 1) have a concave spherical surface to form the cavity and a convex ellipsoidal surface, which provides a straightforward mode matching of a collimated input/output beam to the highly focused cavity mode.[11] The radius of curvature of the concave side is 5.5 mm, resulting in a cavity length $L_C = 2R - d$ in the NC regime, where R is the radius of curvature and d is the (small) critical distance from the concentric point located at $L_C = 2R = 11$ mm. The mirrors have a reflectivity of $\mathcal{R} = 99.5\%$ at $\lambda = 780$ nm, corresponding to a cavity finesse of $F = 627$. The target noise limit factor $\xi = 0.15$ then corresponds to a cavity length fluctuation of $\delta L_{C,rms} \approx 0.9$ Å.

Cavity support structure

To accommodate the cavity mirrors, a structure that allows for adjustment of three degrees of freedom of relative mirror positions is required. Moreover, it needs to fit within the constraints of the vacuum system. In addition, the structure has to have a low susceptibility to external noise. To tackle these limiting factors, a tensegrity structure is chosen.

First, the cavity mirrors are fixed with epoxy to metal mirror mounts [see Fig. 1(b)], which protect the mirrors during handling and shield them from the possible line-of-sight contamination from the atomic source. Gaps at the tip of the shield provide optical access for laser cooling beams to the center of the cavity where the atoms are trapped. The mirrors in their mounts are fixed to aluminum frames. These are separated by piezoelectric actuators (PI PICMA P-882.51) with a rectangular profile, forming the compression members of the tensegrity structure. Different orientations of these actuators with respect to the frames were evaluated.

To implement the tension members, two alternatives are tested. The first alternative used a 0.4 mm thick, laser-cut steel sheet, bent to a clip to hold the two mirror frames together. The clamp is designed such that only three points are in contact with the structure [see Fig. 3(a)]. The second alternative used helical springs (MISUMI AUT3-20), with contact points defined by the hooks of the springs [see Figs. 2(c) and 2(d)].

One of the mirror frames is glued (MasterBond EP21TCHT-1) on a stainless steel plate to avoid applying pressure onto the structure when handling it during installation in the vacuum chamber, while

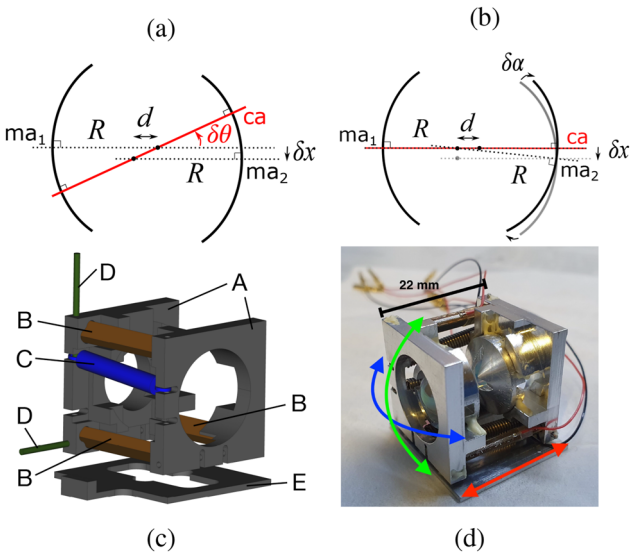

FIG. 2. (a) Rotation of the cavity axis due to transverse misalignment. In a NC cavity of critical distance d, a small transverse misalignment δx of the second mirror rotates the cavity axis by an angle $\delta\theta$. (b) Equivalence of transverse and angular misalignments. A small transverse misalignment δx can be corrected by rotating the mirror by a small angle $\delta\alpha$. (c) CAD drawing: A: mirror frames, B: actuators, C: spring, D: metal rod, E: transportation plate, and (d) assembled NC cavity.

the other frame can move freely in order not to constrain the relative tip–tilt movement of the mirrors.

The piezoelectric actuators have a maximal expansion of 15 μm for an operating voltage of 100 V, sufficient to compensate for misalignment after careful pre-alignment. The transverse misalignment can be corrected via different expansion rates of the three actuators, leading to a relative tip–tilt motion of the mirrors [see Figs. 2(a) and 2(b)]. To allow for independent correction mechanisms for different degrees of freedom, the tip/tilt corrections T_{tip} and T_{tilt} as well as an overall cavity length change ΔL_C are combined to the respective actuator voltages $V_{A,B,C}$,

$$\begin{pmatrix} V_A \\ V_B \\ V_C \end{pmatrix} = G \begin{pmatrix} 1 & 1 & 1 \\ 1 & -1 & 1 \\ 1 & 1 & -1 \end{pmatrix} \begin{pmatrix} \Delta L_C \\ T_{tip} \\ T_{tilt} \end{pmatrix}, \tag{2}$$

where G is a constant representing the transducer gain. This allows for both fast changes of the cavity length and a slower servo mechanism to maintain the transverse cavity alignment.[12]

Different support structure configurations

The small expansion range of the piezoelectric actuators limits the correction range for the transverse misalignment. As large transverse displacements can occur in the cavity structure during the assembly process (epoxy curing and baking of the vacuum chamber), the structure needs careful pre-alignment. A significant aspect of this pre-alignment is the static deformation of the compression structures due to the tension elements and a consequent transverse misalignment. Thus, it is necessary to check and reduce the transverse misalignment resulting from the operation of the actuators.

To evaluate the transverse displacement in the different directions with regard to individual excitation of each actuator, one mirror frame is fixed in place with a clamp, and the displacement of the second mirror frame is measured with a microscope [with a ×10 magnifying objective imaged onto a CCD camera (Point Grey CM3-U3-13S2M-CS)]. The displacements of each structure configuration are listed in Table I. The helical springs show a much smaller transverse misalignment when added to the structure than the flat clip. We believe that this is because the contact points and the static forces of the clips are not as well defined as the ones from the springs, with their spring constant tolerance of ±10%.

Likely due to the actuator's rectangular cross section (2×3 mm^2), an anisotropic bending behavior is observed, with greater flexural deformation along one axis. Rotating the actuators with respect to the frame orientation [see Figs. 3(c) and 3(d)] significantly reduced the transverse displacement (see Table I).

TABLE I. Transverse displacement for several structure configurations.

Structure configuration	Maximum observed transverse displacement (μm)
Clamp [Fig. 3(a)]	3.75
Spring [Fig. 3(b)]	1.25
Parallel base [Fig. 3(c)]	7
45° base [Fig. 3(d)]	3.75

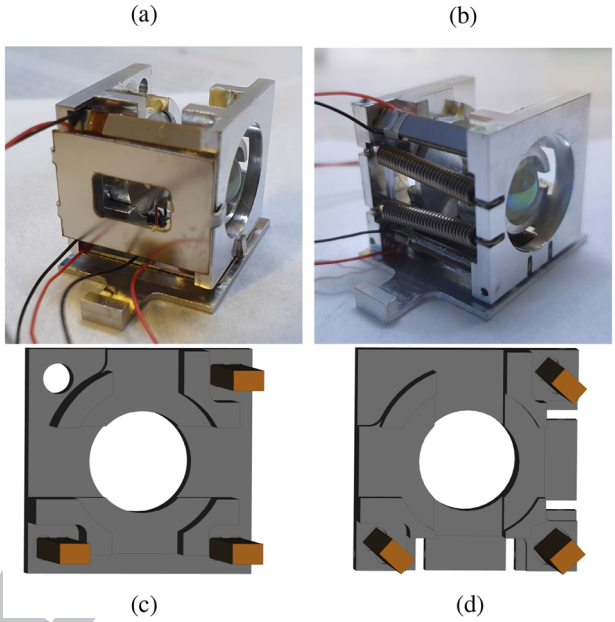

FIG. 3. (a) Structure using a three contact point clamp. (b) Structure using springs. (c) Actuator base parallel to the mirror frame. (d) Actuator base rotated by 45° from the mirror frame.

Cavity alignment

To assemble the near-concentric cavity, a reference axis is established by coupling light between two fiber couplers using four mirrors (see Fig. 4). The cavity system, with the first mirror glued on using a low-outgassing epoxy (MasterBond EP21TCHT-1), is then fixed onto the right tip–tilt stage attached to a three-axis manual translation stage. The combination of the two stages allows the cavity mirror to be freely adjusted along the reference axis. The second mirror is held with a tweezer. The tweezer is also fixed onto the same type of tip–tilt stage as the first mirror, along with a three-axis piezoelectric translation stage with 100 μm moving range (Piezosystem Jena Tritor 101 CAP) for fine adjustment.

By maximizing the coupling of the retro-reflected light from both cavity mirror convex surfaces back into the fiber couplers, each

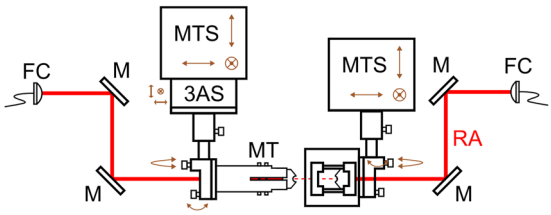

FIG. 4. Alignment setup of the NC cavity. RA: reference axis, FC: fiber coupler, M: mirror, MT: mechanical tweezer, MTS: manual translation stage, and 3AS three-axis actuator stage.

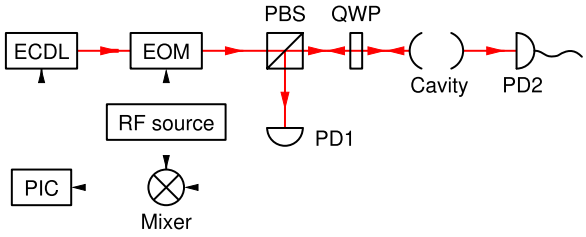

FIG. 5. Schematic of the experimental setup. ECDL: external cavity diode laser, EOM: electro-optical modulator, PIC: proportional integral control, PBS: polarized beam splitter, QWP: quarter waveplate, and PD: photodiode.

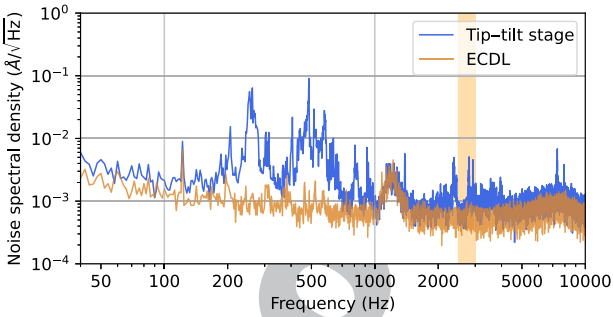

FIG. 6. Noise spectral density of the cavity length over an integration time of 0.5 s. The measurement is conducted at a critical distance of $d = 1.06(5)\ \mu$m for the NC cavity. The total displacement noise is 0.36(2) Å rms. The shaded region highlights the first resonance of the cavity, centered at 2750 Hz (see Fig. 7).

cavity mirror's axis is aligned along the reference axis (see Fig. 4). The second mirror is then slowly translated toward the first mirror to form a cavity mode. The cavity mode and the transmission spectrum of the cavity are observed with a CCD camera and an amplified photodiode (Thorlabs PDA36A2). Any transverse misalignment is corrected using the three-axis piezoelectric translation stage (Fig. 5).

The critical distance d can be estimated from the frequency spacing of the cavity transverse modes. The target critical distance is around $d \approx 7.8\ \mu$m. This value is chosen as it is around half of the travel distance of the cavity's piezoelectric actuators, which will allow a greater tip–tilt tuning as the cavity approaches concentricity.

Once the target critical distance is reached, mirrors are fixed to the frame with a small amount of epoxy such that additional misalignment during the curing process is minimized. During the initial curing of the epoxy (2 h), any misalignment is corrected using the three-axis piezoelectric translation stage. When the epoxy is fully cured after another 70 h, the tweezer is released and removed. The NC cavity is subsequently moved to the glass cuvette using the dedicated transportation plate. This plate, affixed to the cavity stage, directly rests onto the cuvette, which, in turn, is connected to the main vacuum chamber. The vacuum chamber is placed on an optical table stabilized from external vibrations by pneumatic isolators. Due to space constraints in the glass cuvette, the cavity was not mounted on a passive isolation stage, thus remaining susceptible to vibrations transmitted by the vacuum chamber. Any potential noise sources on the optical table, such as cooling fans or loose cables connected to the vacuum chamber, are either powered off, removed, or securely fastened during the measurement process.

CAVITY STABILITY

To characterize the susceptibility of the mounted cavity to external noise, the cavity resonance shift $\delta\omega_C$ is measured with respect to a laser, which is loosely locked to the cavity with a Pound–Drever–Hall (PDH)[15] scheme through an integral controller with a small gain and a sub-Hz cutoff frequency. With this method, fast cavity length changes at high frequencies can be measured, while ensuring that the error signal remains in the linear regime with respect to the length change δL_C, i.e., the mapping to frequency detuning stays injective.

The error signal from the PDH scheme is recorded with an oscilloscope and converted to a length change $\delta L_C(t)$. The noise spectral density of the recorded length change is shown in Fig. 6 for a critical distance of $d = 1.06(5)\ \mu$m, corresponding to three resonant cavity lengths before the concentric point. At this critical distance, the finesse and linewidth of the cavity are measured to be 323(8) and 42(2) MHz, respectively. The root mean square (rms) mechanical noise of the cavity system over the whole spectrum is $\delta L_{C,rms} = 0.36(2)$ Å, or a corresponding frequency uncertainty of $\delta\omega_C = 2\pi \times 1.28(5)$ MHz. Considering one fixed mirror, this rms cavity length change corresponds to a rms transverse displacement of the second mirror of 12 nm.

The recorded error signal combines both laser noise and cavity noise. To separate the two contributions, the laser noise is characterized independently from the NC cavity setup, via modulation transfer spectroscopy[16] using a rubidium vapor cell. The corresponding trace is shown in Fig. 6 as well, with an integral rms frequency uncertainty of $\delta\omega_{laser} = 2\pi \times 0.11(1)$ MHz.

More than 70% of the noise energy of the laser+cavity system is contained in a spectral window between 200 and 2500 Hz, dominated by cavity contributions. This noise contribution could be caused by the susceptibility of transverse vibration modes of the springs to external noise, ultimately coupling to the cavity length.

The analysis above assumes that mode-decoupling from the desired cavity mode due to transverse mirror displacements is negligible during the measurement window. To verify this, we scanned a probe beam to observe the fundamental mode transmission spectrum of the NC cavity and a near-planar cavity with the same support structure separately. We observed no significant difference in the fluctuations of the transmission peak values; thus, we expect cavity resonance shifts to be the main contribution to the noise measurements.

To further enhance the system's stability, one can consider a stronger active stabilization scheme, in addition to the existing loose I lock, for the cavity. This becomes feasible with access to a feedback signal for the cavity length, such as through the PDH scheme mentioned earlier. To implement this, we assess the cavity resonance response to an actuator length change stimulus at different frequencies.

A network analyzer (Agilent E5061b) generates this stimulus, which is added to the actuator's voltage, and picks up the error signal from the PDH scheme in the same loose-lock configuration as above. The resulting Bode diagram of the system response is shown

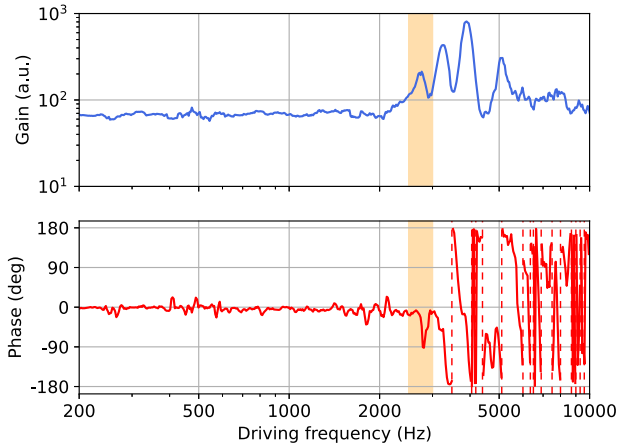

FIG. 7. Cavity response to the stimulus sent to the piezoelectric actuators. The shaded region highlights the first resonance of the cavity, centered at 2750 Hz.

in Fig. 7. A first resonance is observed around 2750 Hz, only contributing 1% of the mechanical noise, with a fairly flat phase response below this resonance. Establishing a phase margin of 60° as the limit of the control for an active stabilization implementation, an active length control of the NC cavity system up to a control bandwidth of ≈2500Hz should be possible, removing the strong broad contribution up to 2000 Hz in the observed cavity noise spectrum. However, in our application, the passive effective cavity length uncertainty of $\delta L_{C,rms} = 0.36(2)$ Å is sufficient.

CONCLUSION

We implemented a passively stable compact structure for a near-concentric cavity, with an effective length uncertainty of 0.36(2) Å at a critical distance of $d = 1.06(5)$ μm. This corresponds to a noise limit factor [see Eq. (1)] of $\xi \approx 0.05$. The passive stability permits an increase in the resonator's finesse while maintaining the cavity's stable relative to its linewidth such that the system can operate effectively close to the concentric point. This increase in finesse will give access to an even stronger atom–light interaction. Implementing an active cavity length stabilization should suppress the susceptibility to external noise even further.

By relying purely on the current susceptibility to the external noise of the cavity system, we can already enter the strong coupling regime with single rubidium atoms with a relatively low finesse of 627. With the current cavity parameters, targeting the D_2 cycling transition of ^{87}Rb, the coupling strength can reach up to $g = 2\pi \times 17.3$ MHz, for a cavity decay rate of $\kappa = 2\pi \times 10.9$ MHz, leading to a maximum cooperativity of $C = g^2/2\kappa\gamma = 4.5$. This strong coupling will be used to explore an atom–light interaction at the last near-concentric stable point.

In summary, we showed that the near-concentric cavity geometry can provide a viable alternative to near-planar cavity geometries for cavity-QED experiments, offering good optical access to the center of the cavity mode for atomic state preparation in quantum information processing schemes and a large separation of mirror surfaces from the mode region with a strong field, reducing, for example, the influence of charges on the mirror surfaces in ion trap configurations.

ACKNOWLEDGMENTS

This work was supported by the National Research Foundation, Singapore, and A*STAR under Project No. NRF2021-QEP2-01-P01/W21Qpd0101.

AUTHOR DECLARATIONS

Conflict of Interest

The authors have no conflicts to disclose.

Author Contributions

Florentin Adam: Conceptualization (equal); Data curation (equal); Formal analysis (equal); Investigation (equal); Methodology (equal); Validation (equal); Visualization (equal); Writing – original draft (equal); Writing – review & editing (equal). **Wen Xin Chiew**: Conceptualization (equal); Data curation (equal); Formal analysis (equal); Investigation (equal); Methodology (equal); Visualization (equal); Writing – review & editing (equal). **Adrian Nugraha Utama**: Conceptualization (equal); Formal analysis (equal); Investigation (equal); Methodology (equal); Software (equal); Validation (equal); Writing – review & editing (equal). **Christian Kurtsiefer**: Conceptualization (equal); Project administration (equal); Resources (equal); Supervision (equal); Writing – review & editing (equal).

DATA AVAILABILITY

■. Q4

REFERENCES

[1] J. P. Covey, H. Weinfurter, and H. Bernien, "Quantum networks with neutral atom processing nodes," npj Quantum Inf. **9**, 90 (2023).
[2] L. J. Stephenson, D. P. Nadlinger, B. C. Nichol, S. An, P. Drmota, T. G. Ballance, K. Thirumalai, J. F. Goodwin, D. M. Lucas, and C. J. Ballance, "High-rate, high-fidelity entanglement of qubits across an elementary quantum network," Phys. Rev. Lett. **124**, 110501 (2020).
[3] Y.-S. Chin, M. Steiner, and C. Kurtsiefer, "Nonlinear photon-atom coupling with 4pi microscopy," Nat. Commun. **8**, 1200 (2017).
[4] C. Hamsen, K. N. Tolazzi, T. Wilk, and G. Rempe, "Strong coupling between photons of two light fields mediated by one atom," Nat. Phys. **14**, 885–889 (2018).
[5] A. Reiserer and G. Rempe, "Cavity-based quantum networks with single atoms and optical photons," Rev. Mod. Phys. **87**, 1379–1418 (2015).
[6] S. Haroche, "Nobel lecture: Controlling photons in a box and exploring the quantum to classical boundary," Rev. Mod. Phys. **85**, 1083–1102 (2013).
[7] J. Ye, D. W. Vernooy, and H. J. Kimble, "Trapping of single atoms in cavity qed," Phys. Rev. Lett. **83**, 4987–4990 (1999).
[8] C. J. Villas-Boas, K. N. Tolazzi, B. Wang, C. Ianzano, and G. Rempe, "Continuous generation of quantum light from a single ground-state atom in an optical cavity," Phys. Rev. Lett. **124**, 093603 (2020).

[9]M. Baghdad, P.-A. Bourdel, S. Schwartz, F. Ferri, J. Reichel, and R. Long, "Spectral engineering of cavity-protected polaritons in an atomic ensemble," Nat. Phys. **19**, 1104–1109 (2023).
[10]Z. Yan, J. Ho, Y.-H. Lu, S. J. Masson, A. Asenjo-Garcia, and D. M. Stamper-Kurn, "Super-radiant and sub-radiant cavity scattering by atom arrays," arXiv:2307.13321 [quant-ph] (2023).
[11]K. Durak, C. H. Nguyen, V. Leong, S. Straupe, and C. Kurtsiefer, "Diffraction-limited Fabry-Perot cavity in the near concentric regime," New J. Phys. **16**, 103002 (2014).
[12]C. H. Nguyen, A. N. Utama, N. Lewty, and C. Kurtsiefer, "Operating a near-concentric cavity at the last stable resonance," Phys. Rev. A **98**, 063833 (2018).
[13]E. L. Raab, M. Prentiss, A. Cable, S. Chu, and D. E. Pritchard, "Trapping of neutral sodium atoms with radiation pressure," Phys. Rev. Lett. **59**, 2631–2634 (1987).
[14]R. Grimm, M. Weidemüller, and Y. B. Ovchinnikov, *Optical Dipole Traps for Neutral Atoms* (Academic Press, 2000), pp. 95–170.
[15]R. W. P. Drever, J. L. Hall, F. V. Kowalski, J. Hough, G. M. Ford, A. J. Munley, and H. Ward, "Laser phase and frequency stabilization using an optical resonator," Appl. Phys. B: Photophys. Laser Chem. **31**, 97–105 (1983).
[16]D. J. McCarron, S. A. King, and S. L. Cornish, "Modulation transfer spectroscopy in atomic rubidium," Meas. Sci. Technol. **19**, 105601 (2008).